U. S. ARMY TEST AND EVALUATION COMMAND
COMMON ENGINEERING TEST PROCEDURE

AERODYNAMIC HEATING

1. OBJECTIVE

The objective of this MTP is to determine the effect of high temperature and temperature changes, resulting from aerodynamic heating, on the missile skin, structure, and interior components using laboratory methods. Such information is used to determine the adequacy of equipment to meet specified requirements such as the ability to withstand the aerodynamic heating associated with flying a specified trajectory.

2. BACKGROUND

Aerodynamic heating is the conversion of kinetic energy into heat energy as the result of the relative motion between a body and a fluid, and the subsequent transfer of this heat energy through the skin into the structure and the interior of the vehicle. Some heat is produced by fluid compression at and near stagnation points, such as the missile nose or the airfoil leading edges. Additional heat results from friction along the missile skin inside the boundary layer. In this area, the relative motion between the fluid particles and the vehicle is reduced by shear force.

Since the advent of high speed vehicles, the effects of aerodynamic heating have been of extreme importance to the design engineer. Frictional heating becomes significant at velocities of approximately 2000 feet per second (fps), which are well within the capabilities of some of the current missiles. It increases the problem of mechanical load distribution of the vehicle, weakening structural members so that more weight is required to withstand a given stress. In addition, thermal stresses further modify the mechanical stress pattern because of the differential in expansion rates for dissimilar materials.

The test engineer must simulate, in the laboratory, many test conditions prescribed either by the designer of the equipment or the military specifications.

3. REQUIRED EQUIPMENT

a. Applicable Testing Facility (convective or nonconvective)
b. Heat Control Computer
c. Applicable Instrumentation (high temperature strain gauges, thermocouples, pyrometers, etc. (as required))
d. Applicable Data Recording and Processing Equipment

4. REFERENCES

A. Miles, Edward R. C., Supersonic Aerodynamics, A Theoretical Introduction, McGraw-Hill Book Company, Inc., 1950.
B. Van Dyke, M. D., Practical Calculation of Second Order Supersonic

33

Flow Past Nonlifting Bodies of Revolution, NACA TN 2744, 1952.

C. Eggers, A. J., Jr. and Savin, R. C., Approximate Methods for Calculating the Flow About Nonlifting Bodies of Revolution at High Supersonic Air Speeds, NACA TN 2597, 1951.

D. Truitt, Robert Wesley, Hypersonic Aerodynamics, The Ronald Press Co., New York, 1959.

E. Tables of Thermal Properties of Gases, National Bureau of Standards, 1955.

F. Low, George M., Boundary Layer Transition at Supersonic Speeds, NACA RM E56E10, 1956.

G. Eckert, E. R. G., Survey on Heat Transfer at High Speeds, WADC Technical Report 54-70, 1954.

H. Stetson, Kenneth F., Boundary Layer Transition on Blunt Bodies with Highly Cooled Boundary Layers, IAS Report No. 59-36.

I. Lees, Lester, Laminar Heat Transfer over Blunt Bodies at Hypersonic Flight Speeds, Jet Propulsion, Vol. 26, No. 4, 1956.

J. Truitt, Robert Wesley, Fundamentals of Aerodynamic Heating, The Ronald Press Company, New York, 1960.

K. Eckert, E. R. G., Engineering Relations for Heat Transfer and Friction in High Velocity Laminar and Turbulent Boundary Layer Flow over Surfaces with Constant Pressure and Temperature, Minneapolis, Minn.

L. Hantzsche, W. and Wendt, H., Die laminare Grenzschicht an einem mit Ueberschallgeschwindigkeit angestroemten, nicht angestellten Kegel, Jahrbuch 1941, der Deutsch. Luftfahrtforschung, Vol. 1

M. Van Driest, E. R., Turbulent Boundary Layer on a Cone in a Supersonic Flow at Zero Angle of Attack, Journal of the Aeronautical Sciences, Vol. 19, 1952.

N. Rubesin, Morris W. and Johnson, H. A., A Critical Review of Skin Friction and Heat Transfer Solutions of the Laminar Boundary Layer of a Flat Plate, Trans. ASME, Vol. 71, 1949.

O. Keenan, J. B. and Kay, J., Gas Tables, John Wiley and Sons, Inc., New York, 1948.

P. Hilsenrath, J., The NBS-NACA Tables of Thermal Properties of Gases, Table 2.44, National Bureau of Standards, 1950.

Q. Eckert, Ernst R. G., Survey of Boundary Layer Heat Transfer at High Velocities and High Temperatures, WADC Technical Report 59-624, 1960.

R. Lin, C. C., Turbulent Flows and Heat Transfer, Princeton, New Jersey, 1959.

S. Korobkin, I., Laminar Heat Transfer Characteristics of a Hemisphere for the Mach Number Range 1.9 to 4.9, Nav. Ord.

T. Jackson, D. W. and Bondurant, R. L., Airframe Structural Integrity Testing - A Challenge in Automation, WADC, 1960.

U. Surface Temperature Measurements with Thermoelectric Materials, Directorate of Engineering Test, WPAFB, Technical Documentary Report No. ASD-TR-61-373, 1962.

V. Kotanchik, Joseph N. and Greenshields, David H., Facilities for High Temperature Flight Environment Simulation, Aerospace Engineering, 1963.

W. Cook, J. C., A 400 KW Pressurized Arc-Image Furnace, South West Research Institute, San Antonio, Texas, 1962.

X. Herczeg, Louis; Yanowitz, Herbert; and Beckman, Paul, Half-Bridge Strain Gage, WADD Technical Report 60-680, 1961.

Y. American Institute of Physics Handbook, McGraw Hill Book Co., Inc., York, Pa., 1957.

5. SCOPE

5.1 SUMMARY

This MTP describes methods of subjecting a test specimen to heating effects that simulate those aerodynamic heating effects that the test specimen would encounter if flown in a given trajectory.

Included in the MTP are methods for mathematically determining the probable heating effects on a test specimen flying a given trajectory using standard air tables, the known trajectory, the shape of the test specimen and known heat transfer constants.

Also included are methods for simulating the above heating effects as a function of time using existing facilities so that the effects on the test specimen from such exposure can be ascertained.

5.2 LIMITATIONS

Due to the variety of missile configurations and trajectory-velocity conditions, no attempt is made in this MTP to describe a testing procedure for any particular missile. The considerations outlined may be adapted as necessary to apply to a given missile and/or flight conditions.

The mathematical considerations presented in the calculation of predicted heating effects, limit this test to simulated temperature and altitudes where conventional gas dynamics solutions are valid or which are in the regime of continuum flow (assumed up to an altitude of approximately 30 to 40 miles) and where dissociation and ionization are negligible. The test is also limited to applications where it can be assumed that there is locally (O) constant temperatures along the surface, zero pressure gradients perpendicular to the missile skin, i.e., $\frac{\partial p}{\partial y} = 0$, and negligible effect due to slip flow.

6. PROCEDURES

6.1 PREPARATION FOR TEST

Personnel involved in testing must be familiar with the missile configurations they are to test, and fully qualified in the use of the associated test equipment and facilities. Prior to the test, pertinent technical manuals, manufacturer's manuals, or other material available must be reviewed to make a proper selection of test equipment and accessories.

The references listed in this MTP contain more detailed information if it is required.

6.2 TEST PROCEDURES

a. Determination of mission profile.

1) Calculate the velocity and altitude of the test specimen as a function of time for the specified trajectory.
2) Using standard atmosphere tables (see reference Y) determine the following free stream parameters for the altitudes determined above: T_∞, ρ_∞, p_∞; and from the velocities: M_∞. (See Appendix A, page A-1).
3) Using the shape of the test specimen, its attitude in flight, and the known free stream parameters, determine the potential flow parameters, T_o, V_o, ρ_o, p_o, and M_o using the references given in Appendix A, page A-2.

4) Calculate the local heat transfer function (h) and recovery temperature (T_r) (as defined in Appendix A, page A-3) as functions of time using the potential flow parameters, heat transfer constants, and the test specimen characteristic length. The material and references listed in Appendix A shall be used to accomplish this.

b. Determine the type of testing facility to be used in conducting the test in accordance with Appendix B.

NOTE: Ensure that the capacity of the testing facility is sufficient to supply the maximum heat flow required.

c. Determine the types of instrumentation and data processing equipment to be used in accordance with Appendix C.

d. Load the heat control computer memory with the values of h and T_r in accordance with Appendix D so that the net heat flow into the test specimen as a function of time will be the same as the test specimen would experience in flying the selected trajectory.

e. Verify, using a data printout or other applicable means, that the values of data stored in the computer memory by the above step corresponds to the pre-calculated values.

f. Place the test specimen into the test facility.

g. Instrument the test specimen to monitor and record wall temperature (T_w), and other desired measurements, e.g., surface strain (See Appendix C)

h. Operate the test facility using the heat control computer to regulate the flow of heat to the test specimen.

NOTE: The onboard equipment shall be operated during the test and any variation from design capabilities shall be noted.

i. Using the test facility instrumentation instead of the test specimen instrumentation monitor the net heat flow into the test specimen.

j. Monitor all test specimen instrumentation data.

k. Shut down the test facility.

l. Remove the test specimen and inspect for any effect of the exposure to the test environment. Record any observations, e.g., degradation of material properties, creep, fatigue, thermal stress.

m. Retain all data recordings.

n. The onboard equipment shall be operated and any variations from design capabilities shall be noted.

6.3 TEST DATA

Retain all data recordings.

Retain all physical observations made on the test specimen after completion of the test.

Retain all observations of the operation of onboard equipment during and after the test.

6.4 DATA REDUCTION AND PRESENTATION

Compare the resultant heating effect with expected values to ensure that test conditions are representative of calculated flight conditions.

From observations made during the physical inspection of the test specimen and from observation made of the operation of onboard equipment during and after the test determine if the test specimen meets manufacturer's specifications and if it is suitable for its intended usage.

GLOSSARY

1. Body of Revolution: A shape generated by a straight or curved line turn-about an axis.

2. Constant Property Values: An equation of property values (heat transfer rate, absolute temperature, pressure, etc.) considered to be constant for purposes of calculation.

3. Continuum Flow: Particle movement in a homogeneous fluid.

4. Conventional Gas Dynamics: A study of fluid in motion.

5. Dynamical Variables: Those variables in terms of which, classical mechanics are built, and which can be given an operational definition.

6. Enthalpy (H): $H = U + pV$, where U is the internal energy of the system, p is the pressure, and V is the volume. At constant pressure, the change in enthalpy is equal to the heat flow into the system from the surroundings.

7. Local Heat Transfer Coefficient (h): h = British Thermal Units divided by the product of time in seconds, area in square feet, and temperature in degrees Rankine.

8. Newtonian Flow Theory: An expression of shear forces in viscous layers, shock detachment parameters, and boundary layer characteristics.

9. Nusselt Number: The nondimensional parameter, defined as $Nu = \frac{Q}{\Delta T} \frac{d}{k}$ where Q is the rate of heat loss from a body, ΔT is the difference of temperature between the body and its surroundings, d is the scale size of the body, k is the thermal conductivity of the surrounding fluid.

10. Prandtl Number: The kinematic viscosity of a fluid divided by its thermal conductivity, $Pr = \frac{C\mu}{k}$.

11. Recovery Factor: A quantity used to specify recovery temperature, and how closely recovery temperature approaches free stream stagnation temperature.

12. Recovery Temperature: In the case of an insulated plate, the equilibrium temperature at which heat transferred out from the inner viscous layer is in balance with the viscous work done on the layers.

13. Reynolds Number: The ratio of the inertia forces to the viscous forces in a fluid, $Re = \frac{\rho V l}{\mu}$.

14. Runge-Kutta Method: A numerical method for solving a differential equation.

15. Slip Flow: One of four distinct flow regimes. In order of increasing

free mean paths, they are continuum flow, slip flow, intermediate flow, and free molecule flow. Information on skin friction and heat transfer in slip flow is limited, and hardly any theoretical results are available for the intermediate regime between slip flow and free molecule flow.

16. Specific Heat: The quantity of heat required to raise the temperature of a unit mass one degree.

17. Stagnation Point: A point at which the velocity of a fluid is zero with respect to a body in motion.

18. State Variables: A limited set of dynamical variables of a system, sufficient to specify the state of the system for given considerations.

19. Static Temperature (wall and free stream): An unchanging temperature which is unaffected by heat from viscous shear.

20. Taylor-Maccoll Equation: An equation to determine the air pressure on the surfaces of cones under conditions of supersonic flow at zero angle of attack.

21. Transition Point: The location on a moving object at which the surrounding fluid ceases to follow the surface, developing eddies and random motion.

APPENDIX A

DETERMINATION OF THERMAL ENVIRONMENT FROM A MISSION PROFILE

In the attempt to solve flow and heat transfer problem for bodies moving at supersonic speeds, the concept of boundary layers has proved to be of great practical value. It permits treatment of extremely complicated actual physical flow fields in two separate parts:

a. Potential flow outside the boundary layer where shear forces in the fluid can be neglected, compared to inertial forces.
b. Boundary layer flow, where shear as well as inertia stress must be considered.

Differential equations describing real physical flow have not yet been solved. Applied to the potential flow fields, however, these equations can be greatly simplified, since shear forces are ignored. The governing equations of the boundary layer are also subject to simplifications, because of a simple flow geometry.

All relationships described in this section of the MTP pertain to conventional gas dynamics or the regime of contiuum flow, assumed to be valid up to an altitude of approximately 30 to 40 miles. The correlations hold true for bodies flying under zero or small angles of attack, with locally constant temperature along the surface, and with zero pressure gradients perpendicular to the missile skin, i.e., $\frac{\partial p}{\partial y} = 0$. Neither problems in slip flow (free molecule flow) nor the temperature regions where dissociation and ionization occur will be discussed.

The prerequisite for engineering calculations of temperatures or heat fluxes resulting from aerodynamic heating is the knowledge of the trajectory of the vehicle to be investigated for any particular mission. From a given flight path, the altitude and velocity of the missile can be established as a function of time for any desired time interval. The required free stream (∞) parameters are extracted from tables of the Standard Atmosphere. (See Reference Y). The parameters are:

V_∞; Vehicle Velocity in feet per second.
T_∞; Atmospheric Temperature in degrees Rankine
ρ_∞; Atmospheric Density in pounds per cubic foot.
P_∞; Atmospheric Pressure in pounds per square foot.

The Mach number can be obtained as: $M_\infty = \frac{V_\infty}{\alpha_\infty}$ (A-1)

where: $\alpha_\infty = \sqrt{MgRT}$

$\alpha_\infty = 49.02\sqrt{T_\infty}$ (velocity of sound in fps) (A-2)

The constant 49.02 renders this equation valid for air only.
If ρ is not available, it can be determined by:

$$\rho_\infty = \frac{P_\infty}{(53.3) \times T_\infty} \qquad \text{(A-3)}$$

(a) Potential Flow Solutions -- The next step is to find the parameter values just outside the boundary layer and behind the shock front occurring on a body traveling at supersonic speeds. These values can be obtained by solving the potential flow equations for the body shape to be investigated. Information on potential flow solutions may be found in References A, B, C, and D. This literature gives solutions of potential flow around cones, ogives and arbitrarily shaped bodies of revolution from low to high Mach numbers. Reference A discusses the potential flow in form of the Taylor-Maccoll equation and its solution in series by iteration. It also explains in detail the methods of characteristics for an axially symmetric supersonic flow.

Reference B contains the calculation of second-order supersonic flow past bodies of revolution at zero angle of attack. The solutions are valid for Mach numbers up to approximately five and for arbitrarily shaped bodies of revolution.

The solution of supersonic flow fields by means of the conical shock expansion method above Mach five is discussed in Reference C. Reference D presents a collection of flow theories including flow over blunt nosed bodies at high velocities. The solutions for potential flow enable determination of the following flow parameters for the station on the missile for which a temperature-time history must be established:

$$\frac{T_o}{T_\infty};\ \frac{V_o}{V_\infty};\ \frac{\rho_o}{\rho_\infty};\ \frac{M_o}{M_\infty};\ \frac{p_o}{p_\infty}$$

With flow values calculated just outside the boundary layer (o), the Reynolds number can be calculated as follows:

$$Re_o = \frac{\rho_o \cdot V_o \cdot l}{\mu_o} \qquad \text{(A-4)}$$

where:

l = the characteristic length in feet
μ = the dynamic viscosity and a function of temperature expressed by a power law given in Reference E:

$$\mu = 0.6729 \times 10^{-5}\ \frac{0.1458 \times (\frac{5}{9}\,T)^{1.5}}{110.4 + (\frac{5}{9}\,T)} \qquad \text{(A-5)}$$

Next, determine whether the boundary layer is laminar or turbulent at the point of investigation. At the present, predictions of the transition point location must be based mainly upon empirical information. Detailed studies are presented in References F, G, H, and I. As a conservative estimate and for engineering calculations, however, assume that turbulent flow exists above a local Reynolds number of 1×10^6 to 2×10^6.

(b) Basic Relationship for Energy Balances and Heat Transfer -- Reference J outlines the heat energy balance and evolving skin temperature equation as follows.

The local heat transfer rate into or out of a surface element of the vehicle is equal to:

$$q_{local} = q_w + q_E + q_N - q_R$$

where:

q = heat transfer rate $[\frac{BTU}{sec}]$

q_w = heat transferred to the skin through the effect of aerodynamic heating

q_E = heat generated by equipment inside the vehicle

q_N = solar and nocturnal radiation

q_R = heat transferred from the boundary layer and skin by radiation

For the domain of operation of the vehicle to be discussed, q_N and q_E generally are negligible compared to the other two terms, and will be omitted in future calculations. Heat dissipation by radiation from the skin is effective only at relatively high temperatures, as shown later in the radiation term. The equation for q_{local} can be written as:

$$q_{local} = q_w - q_R \tag{A-7}$$

or,

$$q_{local} = h\ (T_r - T_w) - \epsilon\sigma T_w^{\ 4} \tag{A-8}$$

where:

h = local heat transfer coefficient $[\frac{BTU}{sec\ ft^2\ °R}]$

ϵ = surface emissivity - dimensionless

σ = Stephan-Boltzmann constant $[\frac{BTU}{sec\ ft^2\ °R^4}]$

T_w = wall temperature [°R]

T_r = temperature of the gas in the boundary layer on the skin surface [°R], when the convective heat transfer at this point is zero.

Conversely,

$$q_{local} = c \cdot s \cdot \delta\ (\frac{dT_w}{dt}) \tag{A-9}$$

where:

c = specific heat of the skin material, $[\frac{BTU}{lb\ °R}]$

s = skin thickness in feet

δ = specific weight of the skin material in pounds per cubic foot

T_w = Wall temperature, [°R]

The assumed conditions are that the inside of the skin is insulated and that all heat energy transferred to the skin from the boundary layer is used to raise the enthalpy of the skin, and that the skin is thin and T_w exists throughout the skin. These conditions do not exist in reality, since part of the heat is transferred into the interior of the vehicle and the temperatures obtained under those restrictions are conservative. The general expression for the local temperature change of the skin with respect to time finally reads:

$$\frac{dT_w}{dt} = \frac{h}{G}\ (T_r - T_w) - \frac{\epsilon\ \sigma\ T_w^{\ 4}}{G} \tag{A-10}$$

where:

G = $SC\delta$= heat absorption capacity of the skin $[\frac{BTU}{ft^2 \; °R}]$

ϵ = surface emissivity [dimensionless]

σ = Stephan-Boltzmann radiation constant and is equal to

$$\sigma = \frac{17.3 \times 10^{-10}}{3600} \; [\frac{BTU}{sec \; ft^2 \; °R}]$$

T_w = wall temperature [°R]

T_r = temperature of the gas in the boundary layer on the skin surface, [°R] when the convective heat transfer at this point is zero

Equation (A-10) is the basic relationship for the change of skin temperatures with respect to time. To this point, the preparatory work holds true for laminar as well as for turbulent boundary layers. From now on, however, laminar, turbulent, and stagnation point heat transfers must be discussed separately.

(c) Heat Transfer in Laminar Boundary Layers -- The main problem of solving equation (A-10) is to determine the local heat transfer coefficient h. In the case of the laminar boundary layer, numerous solutions of the differential equations describe flow and energy conditions in the continuum flow regime. Three of these are presented here from Reference K. They are restricted to two-dimensional flow over surfaces along which the pressure is constant in flow direction. References L and M outline procedures to convert information obtained for two-dimensional flow to conditions on cones. According to these references the local heat transfer coefficient on a flat plate must be multiplied by $\sqrt{3}$ to obtain the local heat transfer on a cone at zero angle of attack for laminar flow. For turbulent boundary layers the local heat transfer coefficient on a cone is found by dividing the cone Reynolds number by 2 and determining the local heat transfer coefficient for the flat plate. This then, is the value for the cone heat transfer coefficient.

(d) Solution for Constant Property Values -- For vehicles traveling in the transonic and low supersonic range, this method is the simplest since the property values (viscosity, heat conductivity, density, and specific heat) are assumed to be constant. As long as the ratio of wall to free stream static temperature lies between 0.5 and 1.5 the results obtained with this method are sufficiently accurate.

This temperature can be obtained through the following relation:

$$r = \frac{T_r - T_o}{T_{t,o} - T_o} = \frac{T_r - T_o}{V_o^2} \, 2 \, C_p \, g \, J \qquad \text{(A-11)}$$

where:

r = recovery factor - see Glossary item 11

g = 32.2 $[\frac{ft}{sec^2}]$ (gravitational acceleration)

T_o = local temperature just outside the boundary layer

J = 778.26 $[\frac{ft \; lb}{BTU}]$ (mechanical equivalent of heat)

$T_{t,o}$= free stream stagnation temperature

Solving for T_r yields:

$$T_r = T_o + r \frac{V_o^2}{50120 \times c_p} \tag{A-12}$$

The recovery factor r can be approximated as the square root of the Prandtl number, so that:

$$T_r = T_o + \sqrt{P_r} \frac{V_o^2}{50120 \times c_p} \tag{A-13}$$

The local heat transfer coefficient h can be expressed in any of the following ways by nondimensional numbers:

$$Nu = \frac{hl}{k} \tag{A-14}$$

$$St = \frac{h}{\rho \, c_p \, V_o} \tag{A-15}$$

$$St = \frac{C_f}{2 \times P_r^{2/3}} \tag{A-16}$$

$$St = \frac{Nu}{R_e \, P_r} \tag{A-17}$$

where:

h = convective heat transfer coefficient, $[\frac{BTU}{hr.\ ft^2\ °F}]$

k = thermal conductivity coefficient, $[\frac{BTU}{hr.\ ft}]$

C_p = specific heat $[\frac{BTU}{lb.\ °F}]$

l = characteristic length in feet

ρ = density $[\frac{lb}{ft^3}]$

V_o = velocity $[\frac{ft}{sec}]$

R_e = Reynolds number

μ = Coefficient of viscosity

P_r, C_f, and N_μ are described in equations A-18, A-20, and A-21.

The Prandtl number is a property value which relates viscosity, specific heat, and thermal conductivity as follows:

$$P_r = \frac{\mu \, c_p}{k} \tag{A-18}$$

As mentioned earlier, the recovery factor r can be approximated as:

$$r = \sqrt{P_r} \tag{A-19}$$

for laminar flow in the range of Prandtl numbers between 0.5 and 5.
The local skin friction factor is

$$C_f = \frac{0.664}{\sqrt{R_e}} \tag{A-20}$$

and the local Nusselt number is

$$Nu = 0.332 \times \sqrt{R_e} \times \sqrt[3]{P_r} \tag{A-21}$$

Substitutions with the parameters discussed enable derivation of the expression for the local heat transfer coefficient:

$$h = 0.332 \frac{c_p \rho V_o}{\sqrt{R_e} \times p_r^{2/3}} \qquad \text{(A-22)}$$

and finally:

$$\frac{dT_w}{dt} = 0.332 \frac{c_p \rho V_o}{G \sqrt{R_e}\, P_r^{2/3}} \left(T_o - T_w + \sqrt{P_r} \frac{V_o^2}{50120 \times c_p}\right) - \frac{\epsilon \sigma T_w^4}{G} \qquad \text{(A-23)}$$

This equation can be integrated by the Runge-Kutta method, since all parameters (once chosen for the corresponding temperature) are constants except the velocity. It simplifies numerical integration if the velocity can be expressed analytically as a function of time.

The advantage of this method is that it depends upon a minimum of parameters and applies in general to any fluid.

(e) Solutions for Proportionality Between μ, k, and T_w -- At higher supersonic velocities, the temperature gradients in the boundary layer perpendicular to the surface are so large, the temperature dependence of the property values must be considered. Heat conductivity and viscosity vary more rapidly than Prandtl number and specific heat. Assuming that P_r and c_p are constant, the following expression shows that the viscosity varies proportionally to the conductivity.

$$\frac{u}{k} = \frac{P_r}{cP}$$

where:

k = thermal conductivity.

Reference N shows that the relations for constant property values can be used, if the temperature dependent property values are introduced at a reference temperature, which is expressed as follows:

$$\frac{T^*}{T_o} = 1 + 0.032 \times M^2 + 0.58 \left(\frac{T_w}{T_o} - 1\right) \qquad \text{(A-24)}$$

This enables performance of the same operations indicated in the preceding paragraph.

f. Solutions for Air with Actual Temperature Variation of all Properties -- The previous considerations were valid for moderately high temperatures in the boundary layer, and it was assumed that the Prandtl number and the specific heat for air were constant. This statement does not hold true for extremely high air velocities where the Prandtl number and specific heat must be considered to be variable also.

Better results are obtained in the calculation of the heat transfer coefficient when the property values and state variables are based on enthalpies instead of temperatures. The use of enthalpies is therefore recommended whenever the temperature variation in the boundary layer is large.

For variable properties, the relationship (A-20) is still valid; i.e., the friction coefficient varies proportionally with the inverse of the square-root of the Reynolds number. However, it is necessary now to introduce the property and state values at a reference enthalpy (i), as defined in the following form:

$$i^* = i_o + 0.50\,(i_w - i_o) + 0.22\,(i_r - i_o) \qquad \text{(A-25)}$$

Results obtained by using this enthalpy formula closely agree with the exact boundary layer solutions. In the Reynolds number μ and ρ must be introduced at i*, and the velocity at V_o. The recovery factor is expressed by equation (A-19) when the Prandtl number is based on the reference enthalpy (A-25).

Values for the Prandtl number, viscosity, and specific heat can be found in gas tables (References E, O, and P). The difference in Prandtl numbers found in reference literature is considerable. Use the tables in Reference E. Using enthalpies instead of temperatures, equation (A-23) now can be modified to:

$$\frac{\partial T_w}{\partial t} = \frac{0.332 \times \rho_r \times V_o}{G \times \sqrt{R_e^*} \times (p_r^*)^{2/3}} \left(i_o - i_w + \sqrt{P_{r^*}}\,\frac{V_o^{\,2}}{50120}\right) - \frac{\epsilon\,\sigma\,T_w^{\,4}}{G} \qquad \text{(A-26)}$$

The density ρ_r is introduced at recovery enthalpy, while all parameters with the superscript* are based on the reference enthalpy (A-25). If the specific heat c of the skin material varies considerably with temperature, the change should be taken into account and all values for c should be chosen at wall temperature T_w.

g. Heat Transfer in Turbulent Boundary Layers -- In contrast to the treatment of laminar boundary layers, the calculation of friction factors and heat transfer coefficient in the turbulent boundary layer is extremely difficult, because knowledge of the turbulent exchange mechanism under widely varying temperatures is limited and experiments must be relied upon.

A comparison between predictions of different theories has shown large differences and therefore a calculation procedure is presented which is recommended in References K and Q and which agrees with experimental results.

The use of the constant property relations in connection with the reference enthalpy method, which was developed for the laminar boundary layer, also can be applied for the turbulent boundary layer.

Schultz-Grunow's equation is used for the skin friction relationship for turbulent flow, as follows:

$$C_f = \frac{0.370}{(\log_{10} R_e)_e^{2.584}} \qquad \text{(A-27)}$$

The recovery factor is represented by an expression similar to that for laminar flow

$$r = \sqrt[3]{P_r} \qquad \text{(A-28)}$$

The determination of the heat transfer coefficient still is based upon equation (A-16) and upon

$$St_i = \frac{h_i}{\rho\, V_o} \qquad \text{(A-29)}$$

where:

$$h_i = h\, c_p \text{ (based upon enthalpy)}$$

All property values must be introduced into equation (A-27) and (A-28) at the reference enthalpy (A-25), and ρ in equation (A-29) at recovery temperature. The recovery factor now is based upon enthalpies,

$$r_i = \frac{i_r - i_o}{V_o^2}\, 2\, g\, J \qquad \text{(A-30)}$$

and the final equation for the temperature change of the skin reads

$$\frac{dT_w}{dt} = \frac{(0.185)(\rho r)(V_o)}{(G)(\mathrm{Log}_{10}\, R_e\, x)^{2.584}\, (P_r*)^{2/3}} \left(i - i_w + \sqrt[3]{p} * \frac{V_o^2}{50120}\right) - \frac{\epsilon\, \sigma\, T_w^4}{G} \qquad \text{(A-31)}$$

This equation can be solved with any of the known integration methods.

g. Stagnation Point Heat Transfer -- Generally, missiles designed to fly at high velocities do not have pointed nose cones nor sharp leading edges, which would have extremely high local heat transfer rates. Instead, noses and leading edges are rounded. Therefore, the two most common forms appearing in missile design (cylindrical and spherical surfaces) are discussed.

(1) Laminar Flow in Stagnation Region -- The expressions describing heat transfer at the stagnation point in laminar flow are described in Reference R. For the cylindrical surface,

$$St_\infty = 0.57 \left(\frac{1}{P_r}\right)^{0.6} \sqrt{\frac{B \times D}{V_\infty}}\ \frac{1}{\sqrt{Re}}\ \sqrt{\frac{(\rho \times \mu)\ Stag}{(\rho \times \mu)_\infty}} \qquad \text{(A-32)}$$

and for the spherical nose

$$St_\infty = 0.736 \left(\frac{1}{P_r}\right)^{0.6} \sqrt{\frac{B \times D}{V_\infty}}\ \frac{1}{\sqrt{Re}}\ \sqrt{\frac{(\rho \times \mu)\ Stag}{(\rho \times \mu)_\infty}} \qquad \text{(A-33)}$$

The property values for equations (A-32) and (A-33) are introduced into the

(a) Prandtl number at stagnation temperature.
(b) Reynolds number at free stream temperature.

The equation for the heat transferred to the wall then is

$$q_w = ST_\infty \times \rho_\infty \times V_\infty\, (i_{stag} - i_w) - \epsilon\, \sigma\, T_w^4 \qquad \text{(A-34)}$$

The term $\sqrt{\frac{B \cdot D}{V_\infty}}$ is described as

$$\sqrt{\frac{B \times D}{V_\infty}}\ \sqrt[4]{\frac{\sigma \times \rho_\infty}{\rho\ stag}} \qquad \text{(A-35)}$$

and since across a normal shock

$$\frac{\rho \text{ stag}}{\rho_\infty} = \frac{(K + 1) \times M_\infty^2}{(K - 1)M_\infty^2 = 2}\left[1 + \frac{K-1}{2} \; \frac{(K-1)\; M_\infty^2 + 2}{2\; K\; M_\infty^2 - (K-1)}\right] \tag{A-36}$$

it follows that

$$\sqrt{\frac{B \times D}{V_\infty}} = \left\{\frac{\delta\;[(K-1)\; M_\infty^2 + 2]}{(K+1)\; M_\infty^2}\left[1 + \frac{K-1}{2} \; \frac{(K-1)\; M_\infty^2 + 2}{2\; K\; M_\infty^2 - (K-1)}\right]^{-\frac{1}{K-1}}\right\}^{0.25} \tag{A-37}$$

Experimental verification for the validity of this equation may be found in Reference E.

Since the Reynolds numbers of the local flow in the vicinity of the stagnation point are low, it is expected that the flow in this region is laminar. In that case, it follows that the maximum heat transfer occurs at the stagnation point.

(2) Turbulent Flow in the Stagnation Region -- With increasing distance from the stagnation point, it is possible that the flow becomes turbulent. For this condition, the following relationship is taken from Reference R.

$$St = A\left(\frac{B \times D}{V_\infty}\right)^{0.8} \cdot \frac{1}{(R_e)^{0.2}} \cdot \frac{1}{(p_r)^{2/3}}\left(\frac{\rho_o}{\rho_\infty}\right)^{0.8}\left(\frac{\mu_o}{\mu_\infty}\right)^{0.2}\left(\frac{X}{D}\right)^{0.6} \tag{A-38}$$

A is a constant having the following values:

A = 0.040 for cylindrical surfaces
A = 0.042 for spherical surfaces, D = diameter of nose

The rate of heat transfer to the wall is:

$$q_W = St_\infty \cdot \rho_\infty \cdot V_\infty\;(i_r - i_W) - \epsilon \cdot \sigma \cdot T_W^4 \tag{A-39}$$

Property values are introduced as follows:

(a) Reynolds number at free stream conditions.
(b) Prandtl number at conditions existing at the outer edge of the foundary layer.

The skin temperature can be calculated in the same way as in preceding paragraphs.

APPENDIX B

AERODYNAMIC HEATING TEST FACILITIES

The three basic modes by which heat can be transferred from one medium to the other are as follows:

Conduction: The heat is transferred as internal energy from one molecule to another. It can occur in solid bodies, fluids, or gases.
Convection: Motions of a macroscopic nature may exist in fluids or gases and the heat is carried along with the motion in form of internal energy.
Radiation: Solid bodies, as well as fluids and gases, can radiate and absorb thermal energy which is transmitted in form of electromagnetic waves.

In technical processes, all three modes of heat transfer usually occur simultaneously with varying degrees of participation for each particular mode.

The methods of heat transfer used in high temperature test facilities can be grouped into two broad categories; nonconvective and convective heat transfer. Reference V presents a detailed description of the various methods and facilities available in these categories, which will be discussed briefly in the following sections.

a. Nonconvective Heating Facilities -- The application of nonconvective heating equipment ranges from small items being tested for material properties to tests of large structural specimens and complete flight vehicles. The purpose of the investigation is to study the effect of high temperature on the degradation of material properties, creep, fatigue, and thermal stresses. These investigations can be performed under a variety of test conditions, such as heating without application of external loads, combined heating and static loading for short and long periods, combined cyclic heating and loading, and programmed heating and loading according to the mission profile. Table B-1 illustrates the capabilities of some of the existing nonconvection heating facilities.

The most widely used method of heat transfer today is the radiant heating method. It resembles the actual process of aerodynamic heating quite well, since it also is a surface heating process. A typical arrangement is shown in Figure B-1. From the consideration of the mathematical description of the physical process two approaches for rapid changes of heat flux have been established. These are: (a) To heat certain elements with a high thermal inertia to a constant temperature. (b) to obtain changes in the heat flux by programming the distance between the test item and the heating elements. A typical heater of this category is the one developed at MIT. It employs silicon-carbon rods ("Globar"-rods) which are mounted on a movable wall of a closed chamber and are resistance-heated to approximately 2800°F with the chamber closed. The wall of the chamber is then swung out to face the test specimen and the desired temperature profile on the test specimen is obtained by programming the distance between test specimen and radiator. (c) To keep the distance between the test specimen and the radiator constant. (d) To obtain rapid changes in heat flux by using heating elements with low thermal inertia and programming the power input to the elements. A typical element of this kind is the quartz tube heat lamp. Because of its versatility and thermal qualities, it is used extensively in the laboratory for simulation of the thermal heat flux of aerodynamic heating.

Table B-1 Capabilities of Nonconvective Heating Facilities

Equipment	Specimen Size (*)	Heating Rate $[\frac{BTU}{sec/ft^2}]$	Temperature Rate $[\frac{deg.\ F}{sec}]$	Maximum Temperature [deg. F]
Radiant heaters Quartz-lamp Radiator	large	150	450 (**)	3,200
Arc Image Furnace	small	2,600	8,000 (**)	7,000
Furnaces	large	-	-	2,000
	small	-	-	5,000
Electrical-Resistance heaters	small	350	1,500	(***)
Induction Heaters	large	3,000	9,000 (**)	(***)
	small	25,000	75,000 (***)	(***)
Electron beam heaters	small	>100,000	>300,000	(***)

Notes:

(*) Large specimens -- typically greater than one square foot of heated surface.
(**) Uniform heating of 0.1-inch-thick aluminum.
(***) Maximum temperature in excess of melting temperature of material.

One of the most commonly used lamps consists of a coiled tungsten wire filament in an argon atmosphere, which is enclosed by a quartz envelope of 0.375 inch diameter. The lamps can be assembled in arrays of different configuration to fit the shape of a particular test specimen. For maximum thermal flux, the lamps are closely spaced in each of two rows, where one row is placed behind the other in such a manner that the filaments of the back row lamps fill the spaces between the filaments of the front row lamps. Heating rates that a are attainable with quartz lamp heat radiators are about 150 $[\frac{BTU}{sec.\ ft^2}]$, with

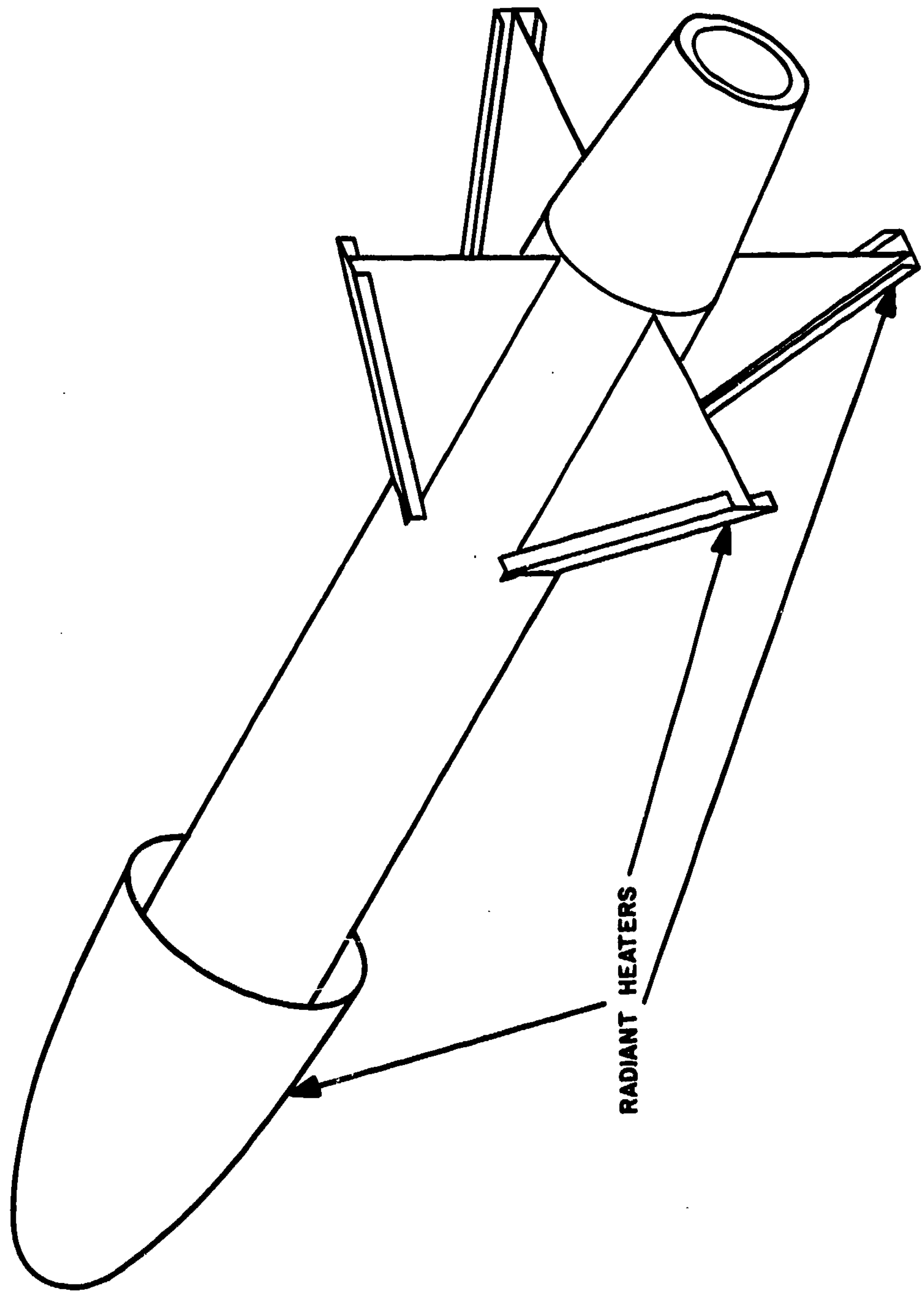

FIGURE B-I. ACRODYNAMIC HEATING SIMULATION cylindrical radiators.

The lamps are available in various lengths from 5 to 50 inches with two types of filaments with power ratings of 100 and 200 watts per inch at the rated voltage. They can also be operated on a short time basis at 100 percent overvoltage and then deliver 300 and 600 watts per inch, respectively.

The thermal inertia of the quartz tube lamps is small, therefore, the thermal flux can be varied rapidly and accurately. The type of radiator control widely in use today is the ignitron, which has fast response and which is adaptable to a wide range of electrical loads.

The thermal capabilities of cooled and uncooled quartz lamp heat radiators are compared with the thermal simulation requirements of ICBM and manned reentry vehicles in Figure B-2, which also were taken from Reference V. As shown, quartz lamps can generate the thermal requirements for a large portion of the manned vehicle environment, but are inadequate for ICBM simulation. For this portion of the diagram, which required heat transfer rates substantially greater than those available from quartz lamps, the arc-image or solar furnace is used.

In the arc-image furnace, radiation from the hot gases in the anode crater of a carbon arc is utilized to achieve heating rates of several thousand BTU/ft^2 sec. The application of arc-image furnaces is limited, however, because the area which can be irradiated is too small for the purpose of thermal testing of aerodynamic configurations. The radiant heating rates can be increased by operating the carbon arc in an elevated pressure atmosphere, and fluxes of 2600 BTU/ft^2 sec have been reported. Reference W provides more detailed information.

The greatest usefulness for conventional furnaces, including arc-image furnaces is in the field of materials research. They are not suitable for applications in which temperature gradients are important. Lower temperature furnaces (to 2000 degrees Fahrenheit) usually can accommodate small test items, while higher temperature furnaces generally are of a tubular design and restrict specimen size and shape.

In the category of electrical resistance heaters, it is necessary to distinguish between two types of heating equipment; one which directly heats the specimen by utilizing the specimen's electrical resistance, and one which indirectly heats the test item through the use of a resistance heated blanket in direct contact with the specimen. The latter method is obsolete, whereas the direct resistance heating technique is widely used for testing metallic materials.

The main advantage of induction heating is its ability to develop high heating rates and temperatures in the test item. However, in contrast to radiant heating, induction heating is not a surface phenomenon. Depending upon the frequency of the heating current and the resistivity of the material, the heating is concentrated at a certain depth below the surface. In addition, the

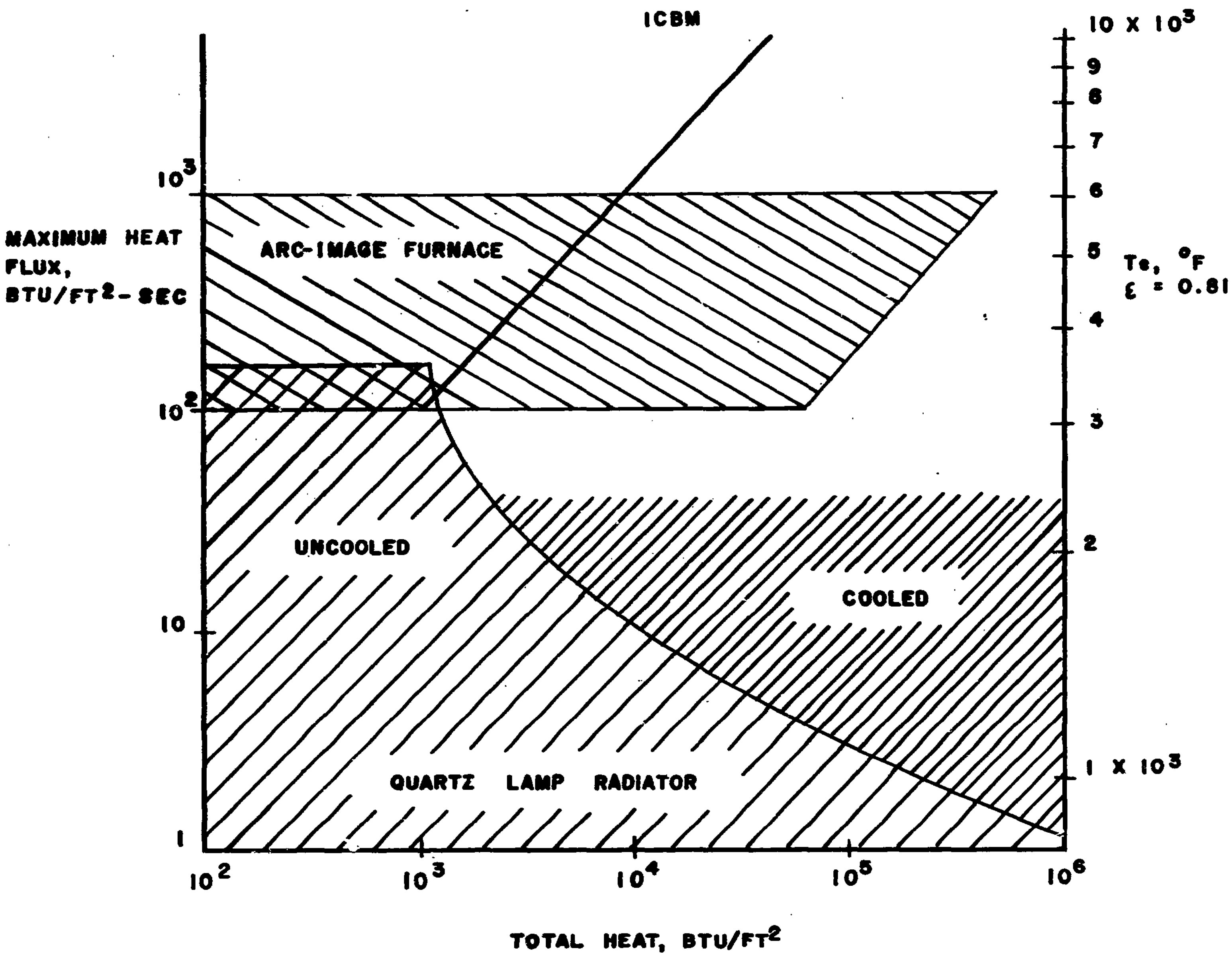

FIGURE B-2. THERMAL SIMULATION CAPABILITY OF TWO TYPES OF RADIANT HEATERS practical application of induction heating for aerodynamic heating simulation is limited by the physical arrangement of the heating coils.

Heat transfer rates in excess of 100,000 BTU/ft^2 sec have been obtained over small areas by bombarding the surface with a direct beam of electrons. The technique is relatively new and its full usefulness in the simulation of aerodynamic heating has not been determined.

b. Convective Heating Facilities -- Convective heating bears the closest resemblance to actual aerodynamic heating. It is possible to achieve duplication of true velocity, enthalpy, and heat transfer rates in large facilities for simulation of low supersonic velocity flight. In the region of high supersonic and hypersonic flight simulation, the size of the test specimen and the duplication of parameters are restricted. Table II illustrates some of the existing convective heating facilities.

Table II. Capabilities of Convective Heating Facilities

Facility	Specimen Size (*)	Heat Transfer Rate $\left[\frac{BTU}{sec/ft^2}\right]$(**)	Stream Enthalpy $\left[\frac{BTU}{lb}\right]$	Total Temperature [deg. F]
Resistance heated Tunnels	small	55	550	2,200
Ceramic heated Tunnels	small	300	1,100	4,000
Combustion heated Tunnels	large	180	1,400	4,000
Electric heated arc facilities	small	1,000	18,000	16,000

Notes:

(*) Large Specimen-typically greater than one foot in diameter.
(**) To models of one-inch hemispherical radius.

For a moderate range of velocities, the energy in the air stream of a supersonic tunnel can be supplied from resistance heated heat exchangers. The maximum operating temperature of materials of the heat exchangers limits the range of operation to 2000 degrees Fahrenheit for stainless steel and 2500 degrees Fahrenheit for Kanthal (Swedish iron alloy). A heat exchanger of the latter type exists at Langley Research Center in a continuous flow Mach 12 tunnel and provides a stream with a total temperature of 2,250 degrees Fahrenheit.

In a current development effort, porous carbon is heated to 5000 degrees Fahrenheit and nitrogen is passed through it at low velocities to permit heat absorption without erosion of the carbon. The nitorgen may be used as a test medium or oxygen, heated separately in a metallic heat exchanger, may be added downstream of the carbon heat exchanger to provide synthetic air at temperatures substantially higher than can be obtained from metallic heat exchangers alone.

Ceramic heated tunnels provide another technique for obtaining high temperatures in wind tunnel air streams. The ceramic bed consists of pebbles of aluminum oxide, zirconia, or other ceramic high temperature materials. High temperature combustion gases are passed through the bed until the pebbles attain the desired temperature. Compressed air then is blown through the ceramic bed, heated to high temperature, and expanded through a nozzle to high supersonic velocities. Temperatures achieved with a large version of the ceramic heated air jet were approximately 4000 degrees Fahrenheit. A serious drawback of ceramic heated facilities becomes evident after some period of operation. The cyclic heating fractures the pebbles and the high temperature air stream becomes contaminated with ceramic dust particles, which in turn, erodes the test models.

Combustion provides an economical means of heat addition to a gas stream. A slight deficiency, however, is the presence of high temperature combustion products instead of high temperature air. This can be circumvented by using fuels which yield products of combustion with properties approximating those of air. An advanced type of facility employing combustion heating is the high temperature structures tunnel at the Langley Research Center. Natural gas or ethylene is burned in a high pressure combustor and the combustion products are expanded to a velocity of Mach 7 with stagnation temperatures to 4,000 degrees Fahrenheit. The stream of combustion products contains 79 percent Nitrogen, water vapor up to 10 percent, oxygen, and carbon dioxide. The power in the stream is approximately one gigawatt (10^9 watts).

Another facility at the Langley Research Center is a 9- by 16-foot tunnel which employs combustion of a fuel as the source of heat energy, but the energy is transported to and stored in a stainless steel heat sink. Compressed air is then passed through the sink and heated to 600 degrees Fahrenheit. Although this is a moderate temperature, the tunnel is capable of developing true aerodynamic heating and loading of Mach 3 speeds at 35,000 feet altitude on relatively large models.

A major breakthrough in the effort to increase the energy in air streams of ground facilities was the use of electric arcs to heat the test medium. Although a great extension of the simulation capabilities of wind tunnels was achieved, arc heated facilities as yet do not provide complete simulation over the entire flight region. Because of disassociation and ionization in high temperature air, the pressures required in the arc chamber to produce gas streams of reentry Mach numbers become impracticably high. As a result, arc heated chambers can produce convective heat transfer rates of over 1,000 BTU/ft^2 sec and enthalpies of 18,000 BTU/lb in air and can thus simulate these parameters over most of the flight regions for manned and unmanned vehicles, although flight Mach number simulation must be omitted.

To provide simulation at positions on reentry bodies other than the stagnation region, more sophisticated techniques have been developed in which the manipulation of subsonic or low supersonic streams provides laminar or turbulent flows and simulates changes in heat transfer rate and flow velocity over extended regions away from the stagnation point.

c. Recent Developments -- Two recent developments in the areas of radiative and convective heating offer promise of high gas velocities and high radiant energy fluxes. They are the magneto-gasdynamic accelerator and the laser, which are still in their initial development stages and not yet suitable for high-power application.

The operating principle of the magneto-gasdynamic heater is to accelerate ionized gases, such as those produced by a conventional arc-heater, by a body force applied to the charged particles in the stream. As a result, the gas is accelerated in a given direction without a significant increase in static stream temperature. Theoretically, this device could accelerate the gas to any desired velocity; however, experiments show that it is difficult to increase the stream velocity by orders of magnitude without employing tremendous amounts of energy.

The laser is a source of nonthermal radiation in which most of the energy is emitted as a coherent beam of radiant energy which can be focused on a spot of extremely small size. Radiant energy flux densities in the spot surpass everything that has been obtained so far in the laboratory.

APPENDIX C

INSTRUMENTATION

A. High Temperature Measurements -- Temperature measurements on a metallic test specimen can be performed with a reasonable degree of accuracy by thermocouples up to approximately 2000 degrees Fahrenheit. Above this limit, thermocouple measurements become more difficult and less accurate. Reference U presents a detailed study of errors in surface temperature measurements made with thermocouples, when both the thermocouple wires and the surface are exposed to radiant energy. The dependency of accurate results upon various parameters is discussed and recommendations are made for the proper use and installation of thermocouples.

For higher temperatures, various types of pyrometers are suitable for measurement of a steady-state environment, but become less accurate as the temperature rate increases.

B. Strain Measurements at High Temperatures -- One of the important aspects of the structural behavior of a test specimen is the measurement of strain. Techniques for conventional strain gages (installation and measurement) are well established for a normal temperature environment, but become exceedingly difficult at temperatures above a few hundred degrees Fahrenheit. At these temperatures, special techniques are employed to measure strain; for instance, optical measurements of displacement of reference marks on the heated surface, off-surface strain gages, measurements on the cold side (if available) of a test specimen, or the half-bridge strain gage described in detail in Reference X. The principle underlying the operation of the half-bridge strain gage is to induce theoretically equal temperature effects in each component of a half-bridge which cancel when the elements are connected in a standard wheatstone bridge circuit. Solutions are developed for the compensation for effects such as thermal coefficient of resistance of the strain-sensitive wire, the self-heating of the gage caused by the electrical current flowing, the strain sensitivity of each arm, leakage resistance of the cement, and the lead resistance.

C. Gas Property Measurements in Convective Heating Facilities -- The use of convective heating facilities requires the measurement of additional parameters related to the properties of the gas stream. These parameters are the enthalpy, velocity, and pressure of the gas and the heat transfer rate experienced by the test specimen. They are discussed under "Measurements in Arc-heated Air Streams" in Reference V. According to this reference, pressures easily can be measured using standard pressure transducers. Probes used for dynamic pressure measurements must be water cooled. Velocities can be measured directly or can be calculated from pressure and temperature data. Mach numbers can be obtained by reading photographs of the shock waves formed on wedges immersed in the gas stream.

Several methods have been used successfully for obtaining the surface heat transfer rate which is one of the most important parameters in high temperature testing. The simplest form of such a measuring device is a thin metallic disk with a thermocouple attached to the center. When the disk is immersed in the gas stream, the rate of temperature rise is a direct measure of the heat transfer rate.

For the measurement of stream enthalpies and temperatures, several direct and indirect methods have been developed. The gross enthalpy may be determined by measuring the total flow weight and total energy of the stream. The latter can be calculated by subtracting the energy lost in the arc apparatus from the total power input to the arc heater. Another way to determine the total energy is to collect the entire gas stream in a tube and measure the energy absorbed by the tube in cooling the gas. A useful, indirect method for determining the enthalpy or temperature as a function of position in the stream is based on the heat transfer rate theory of Fay and Riddell. Stagnation point heat transfer rate on a body is calculated as a function of stagnation enthalpy and density, and local velocity gradient. Newtonian flow theory is used to calculate the velocity gradient in supersonic flow, whereas in the subsonic region, potential flow theory is applied. Results are meaningful only for Reynolds numbers above 1000.

Another direct measurement of enthalpy at particular locations in the stream can be made by using a small gas sampling probe which draws off a measured weight flow. The enthalpy is determined from the heat extracted in the probe.

Spectrophotometry is one of the methods used in the direct measurement of stream temperatures. It utilizes the spectral intensity distribution of energy radiated by the stream and it generally yields temperatures indicative of one degree of freedom of the gas. These temperatures describe the energy state of all components in the gas, provided the gas is in thermodynamic equilibrium.

D. Data Handling Equipment -- In dynamic test applications, the rapid collection, reduction, and interpretation of data is essential to the successful completion of the program. This can be accomplished only through the use of automatic electronic data handling equipment. Various types of automatic data processing equipment are available, but it would exceed the scope of this section to discuss all of them in detail.

The important aspects for the acquisition of a data handling system as presented in Reference T are listed as follows:

a. Sufficient channel capacity and sampling speed, in the commutated mode, to support test requirements ranging from static loading with steady-state temperatures to dynamic transient loadings and temperature with the option of sacrificing channel capacity for increased sampling rate.

b. The capability of programming the system to operate in a fully automatic mode when events are occurring so rapidly that human perception or judgement cannot be applied.

c. System accuracy such that the transducers contribute the major sources of error.

d. Data editing capabilities so that data can be examined for its informational content prior to machine processing.

e. Modularization so that a part of the system may be used to obtain data from one test article concurrently with test setup operation of the remainder of the data system on a second or third article.

f. Isolation capabilities such that transducer failure or malfunction on one channel will not affect the operation or accuracy of any other channel.

g. The capability of processing and putting out a large volume of test data within a short period of time for examination and analysis by instrumentation engineers.

h. Sufficient growth capacity such that the system will not become obsolete within a reasonable time period.

i. Component or module accessibility for setup and maintenance purposes.

To show the capability of typical system, the description of the WADD elevated temperature and fatigue test facility data handling system is quoted from Reference T: "This system collects (by commutation and with a variable sampling rate), records, analyzes, reduces, displays, and stores the outputs of various sensing devices such as strain gages, load cells, deflection potentiometers, and thermocouples. Electrical signals from the transducers are detected, conditioned, and transmitted by shielded cables to a data control and processing area. Here the data are visually monitored, recorded on magnetic tape, processed and stored by means of a large scale digital computer and a high-speed printer-plotter. Also included are 'limit-alarm' and 'quick-look' display features.

"The system consists of eight transmitter-multiplexer units, two monitor consoles, four one-inch tape recorders, four one-half inch tape recorders, one system control console, a large scale digital computer and a high-speed electronic printer plotter.

"Total channel capacity, for the full scale system, is 1920 channels. A basic block diagram of the full scale system is shown in Figure C-1. The channel capacity can be increased by simply adding transmitter-multiplexer and tape recorder units."

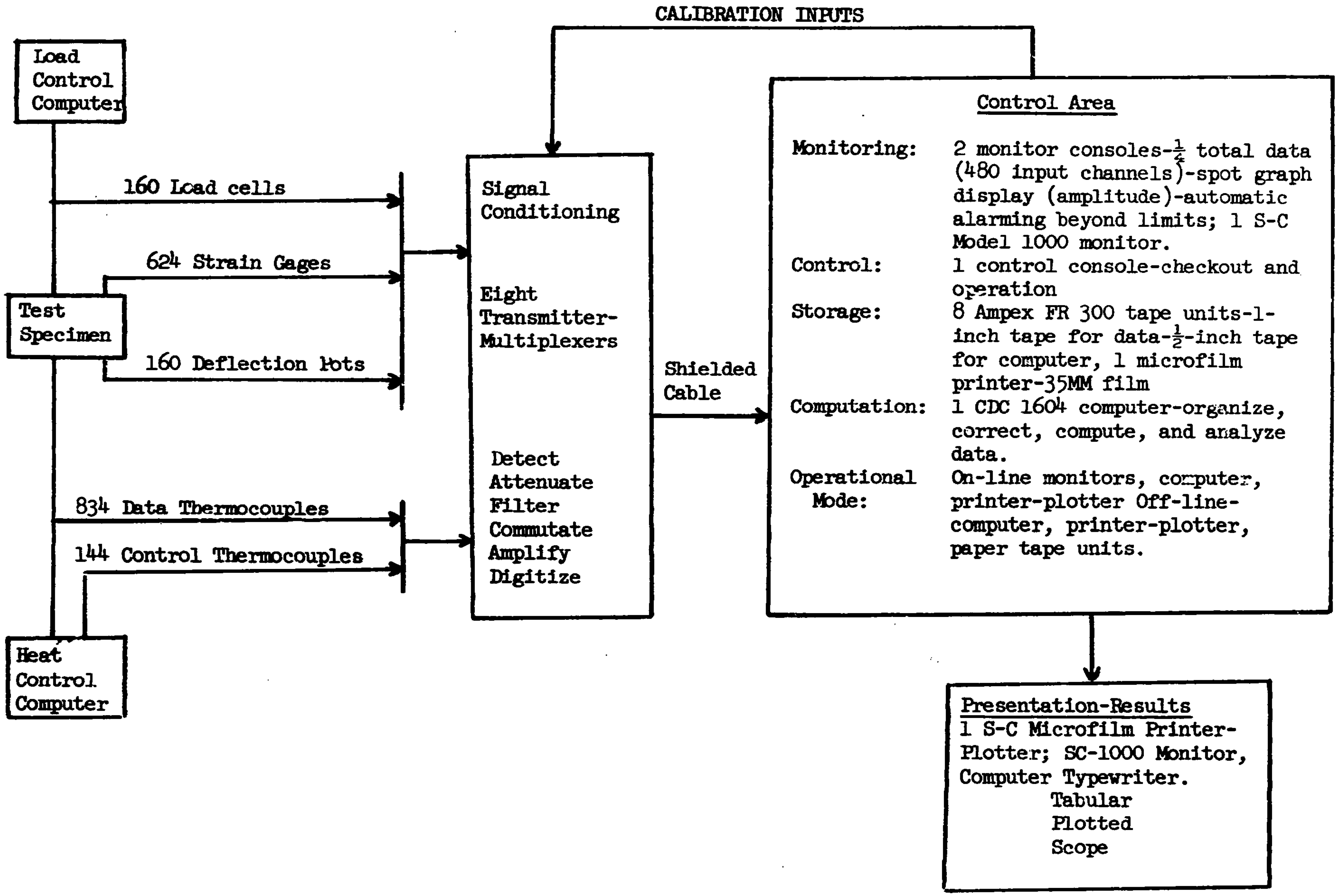

Figure C-1 Data Handling System Block Diagram

APPENDIX D

BASIC TECHNIQUES FOR PROGRAMMING MISSION PROFILES

The basis for programming thermal profiles is equation (A-8), which is solved by a heat control computer. The principle of operation is demonstrated through the use of a radiant heating test facility, although basically it applies to different types of heating equipment.

a. Heat Control Computer Purpose -- The purpose of the heat control computer in conjunction with electrical power control equipment (ignitrons) is to regulate the heat applied to test structures to duplicate the effect of aerodynamic heating resulting from flight at supersonic speeds. The method of operation presented here is taken from Reference T, which describes part of the radiant heating facility at Wright Air Development Division (WADD).

The calculation procedures in Appendix A show that the analytical determination of the instantaneous specimen temperature T_W is tedious. As used in the computer facility, it is an actual test derivative from the control thermocouple for the test area under consideration rather than by calculation. For test purposes, the variation of the heat transfer coefficient h and the recovery temperature T_r with respect to time are required. The remaining items are known for a specific test article and the given test conditions. Equation (A-8) can be written in a different form, as follows:

$$q_{local} = c \cdot s \cdot \delta \cdot \frac{dT_W}{dt} = h\,(T_r - T_W) - B\,T_W^4$$

where: $B = \epsilon \cdot \sigma$ (a constant for a specific test article)

Further, the thermal input can be related to the power input of the laboratory heat source by

$$Q = Y \times E \times I \times 10^{-3}$$

where:

Q = heat produced in the electrical process
Y = a constant relating KW to BTU/sec
E = load voltage
I = load current

Reference T states, "The heat control computer solves equation (A-8) instantaneously using as inputs the precalculated values for the recovery temperature T_r and the heat transfer coefficient h together with the measured surface temperature of the test structure T_W. The generated output signal controls the heat source to produce the proper heat flow rate Q."

b. Computer Operation -- A functional block diagram of a forty-channel heat control computer is shown in Figure D-1 (Reference T). Curves are plotted from the precalculated input data. Three hundred points for each of ten recovery temperature T_r curves and forty heat transfer coefficient h curves are punched in a seven place code on paper tape and transferred in digital form by means of tape reader and write circuitry to a magnetic storage drum. Through use of the read circuitry, each curve can be plotted on a strip chart recorder to verify visually the accuracy of the information that is stored on the drum. The read circuitry scans points of equal abscissa from the curves during each drum revolution as programmed by a time base selector. Although the time base range covers thirty seconds to one hour in increments of 10 seconds, the scanning may be held at any of the abscissas up to eight hours. The digital outputs of the read amplifiers are converted to analog voltages by means of D-A converters. The forty h curves are applied, through the converters, directly to a high speed rotary multiplexing switch. The ten T_r curves are applied, through the converters, to forty ten-position switches. The selector arm on these switches is in turn applied to the multiplexing switch, thereby allowing one of ten possible T_r temperature selections to be used for each of forty test areas.

Temperature input is derived from a thermocouple through a low level thermocouple amplifier circuit. In addition to amplification, the thermocouple is linearized so that its output signal is proportional to temperature. A thermocouple test circuit is available to test the operation of each thermocouple channel. Thermocouple failure circuits, connected to the low level amplifiers, indicate any open circuit in the thermocouple input circuits. The radiation factor $B = \epsilon \cdot \sigma$ is set manually for each channel.

The signals which represent T_r and $- T_w$ are summed in amplifier number 1. The output signal of this amplifier is modified by the signal representing h in the multiplier. The multiplier output is a voltage proportional to $-h\ (T_r - T_w)$. The representative signal $- B^4 \cdot T_w$ is applied to the input of the function generator to produce a signal proportional to BT_w^4. The signals $- h\ (T_r - T_w)$ and BT_w^4 are added in summing amplifier number 2 and the output represents $h \cdot (T_r - T_w) - BT_w^4$ which is proportional to the desired power Q. This output is commutated by the multiplexing switch to the output holding circuits. A combined area and heat transfer efficiency factor, K, is introduced and this output is compared with either the rate of temperature rise ($c \cdot s \cdot \delta \cdot \frac{DT_w}{dt}$) or the power consumed ($Y \cdot E \cdot I$) feedback loops (depending upon the mode of operation) in summing amplifier number 3. The resulting signal is used to control the power to the heat source.

In the $c \cdot s \cdot \frac{dt_w}{dt} \cdot \delta$, or derivative feedback mode, a signal from the thermocouple linearizer is differentiated. This constant $c \cdot s \cdot \delta$ is set in and the signal is entered in amplifier number 3. In the power feedback mode, signal voltages representing the voltage and current in the lamps are multiplied to produce a signal which represents the power used by the lamps. This signal is averaged by a filter network to represent the actual power per cycle. The output of this network is modified by the constant conversion Y and is sent to summing amplifier number 3.

If the wall temperature-time history of the test items has been established, then the h curves may be substituted by the T_w curves in this mode of operation. (See Figure D-2) The signals representing T_w are fed directly from the D-A converter to the output holding circuit. T_w is multiplied by K and the signal KT is then compared with the actual value of T_w amplifier and fed through $c \cdot s \cdot \delta$. The generated error signal controls the power units.

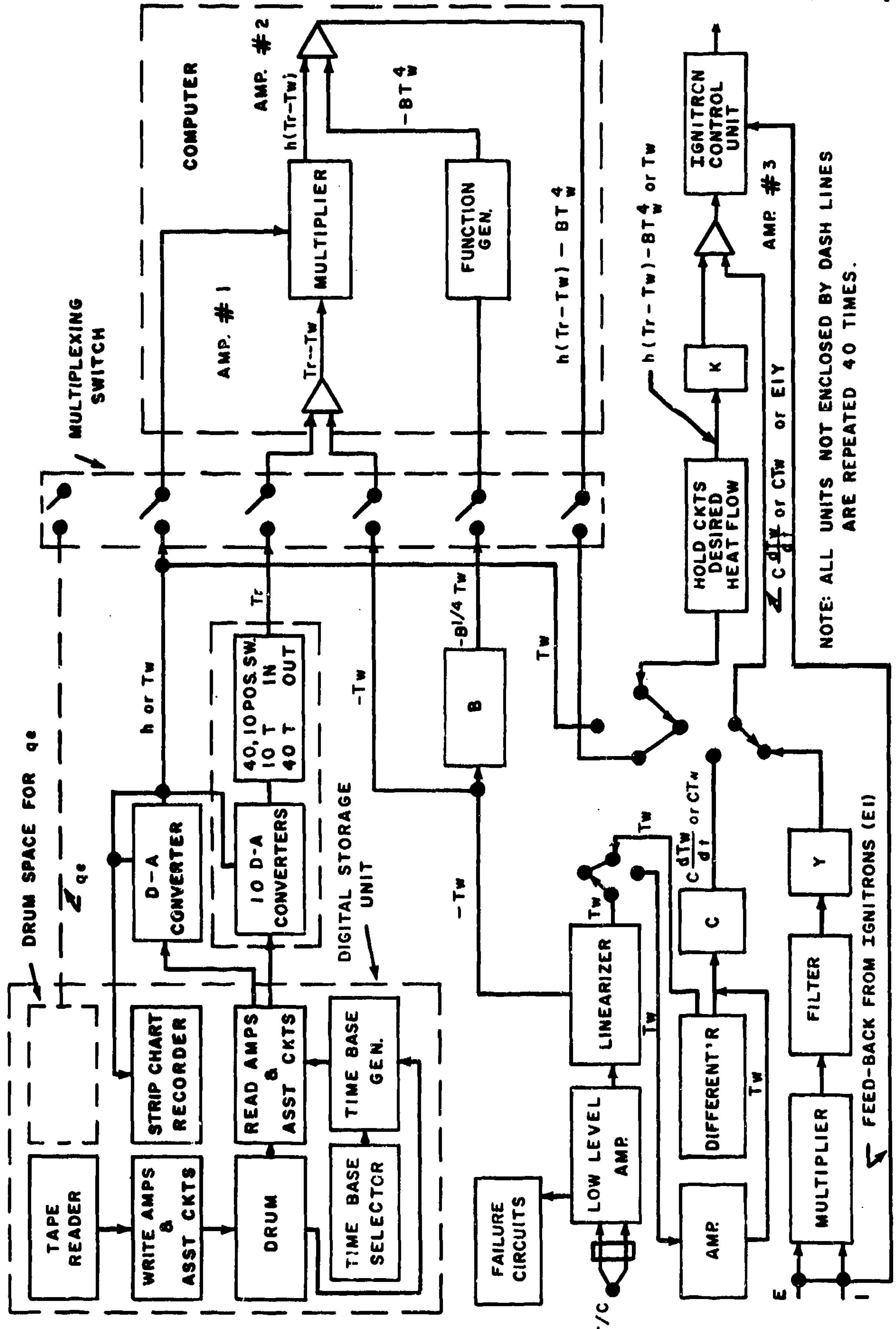

FIGURE D-1. FUNCTIONAL DIAGRAM OF WADD (G.E.) 40 CHANNEL HEAT CONTROL COMPUTER

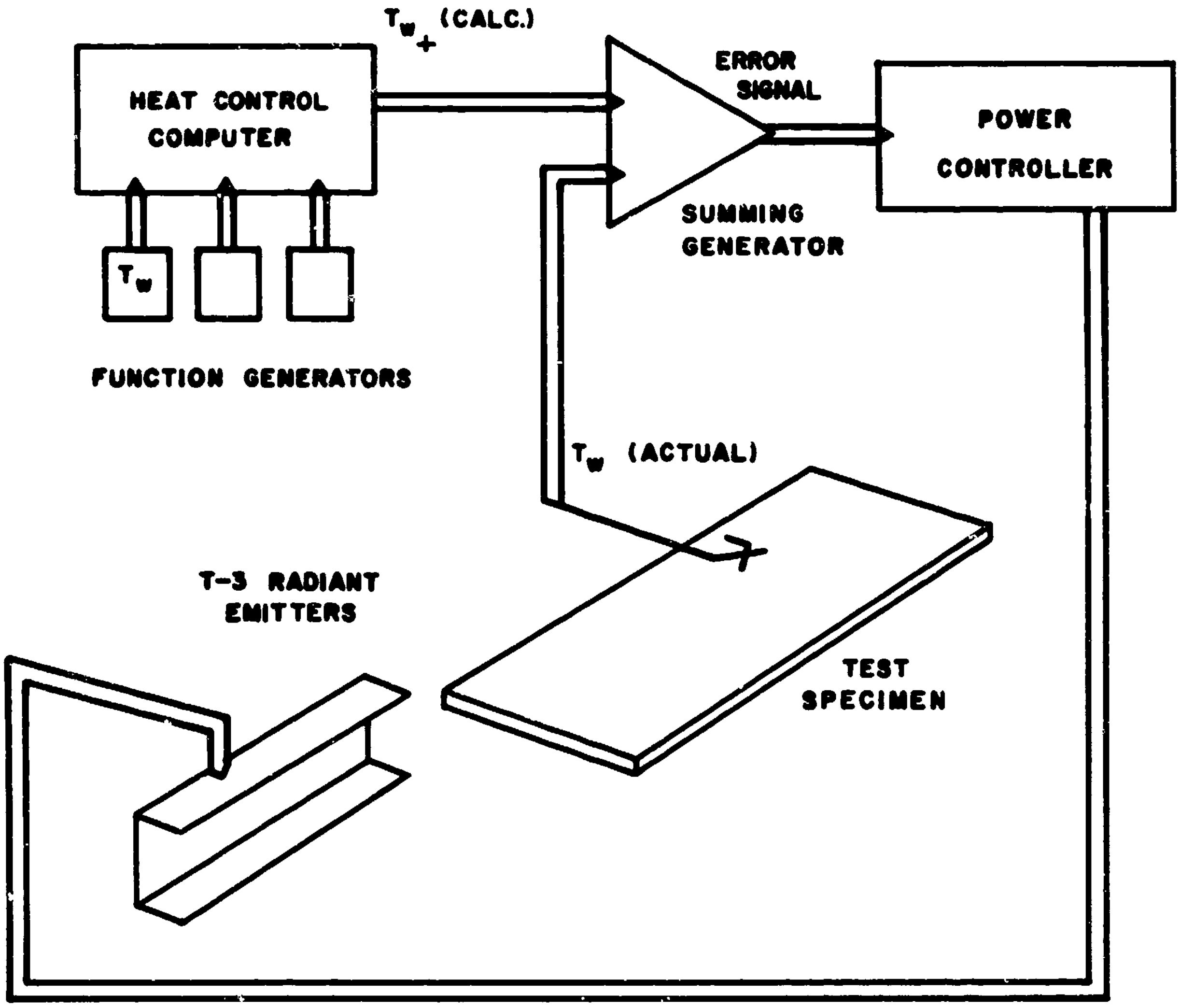

FIGURE D-2. TEMPERATURE VERSUS TIME CONTROL ARRANGEMENT